

# EFFECTS OF SPATIAL VARIABILITY OF SOIL PARAMETERS ON THE DIFFERENTIAL SETTLEMENT AND THE INTERNAL FORCES OF A FRAME STRUCTURES

Mohamad Nazieh Jilati  
Widener University, Chester, PA, USA



Challenges from North to South  
Des défis du Nord au Sud

## ABSTRACT

One of the distinguishing features of geotechnical reliability analysis, compared to other structural reliability analysis such as concrete and steel structures is material properties are different from site to site. The sources of uncertainties in reliability analysis are usually classified in four categories, namely physical uncertainty, model uncertainty, statistical uncertainty and gross error.

The purpose of this study is to quantitatively evaluate the impact of physical uncertainty of soil on the differential settlement of circular shallow foundations on statistically homogeneous elastic ground and the stresses in a 1<sup>st</sup> degree indeterminate frame structures. The settlement and the differential settlement were predicted; the stresses had not exceeded 1.2 % increment of the homogenous conditions in the studied frame structure.

## RÉSUMÉ

L'analyse de la fiabilité en géotechnique est complexe car les propriétés des matériaux sont différentes d'un site à l'autre, ce qui n'est pas le cas pour d'autres analyses de fiabilité structurale, telles que pour les structures métalliques ou en béton. Les sources d'incertitudes dans l'analyse de fiabilité sont habituellement classées en quatre catégories, à savoir l'incertitude physique, l'incertitude du modèle, l'incertitude statistique et l'erreur brute.

Le but de cette étude est d'évaluer quantitativement l'impact de l'incertitude physique du sol sur le tassement différentiel de fondations circulaires peu profondes dans un sol élastique statistiquement homogène et sur les contraintes dans une structure hyperstatique de 1er degré. Le tassement et le tassement différentiel ont été prédits; les contraintes n'ont pas dépassé 1,2% par rapport aux conditions homogènes dans la structure de charpente étudiée.

## 1 INTRODUCTION

In many of the textbooks in reliability design, the sources of uncertainties are classified in four categories, namely physical uncertainty, model uncertainty, statistical uncertainty and gross error (e.g. Thoft-Christensen and Barker, 1982). In the actual situation, it is observed that it is a combined result of all of these uncertainties. For example, there are differences between the accuracy of the prediction of the settlement of shallow foundations or the internal forces and the observations, and it is practically impossible to quantitatively identify each one of the four sources separately.

Fenton and Griffiths (2002), Honjo et al. (2007), and others have studied the influence of the spatial variability on the settlement prediction. However, one may not find any research discussing the relationship between the spatial variability of soil and its effect on the structures.

## 2 Objective and scope

The objective of this study was to quantitatively evaluate the physical uncertainty impact on the internal forces of a frame (*i.e.* spatial variability of soil properties) based on by the differential settlement prediction of flexible circular shallow foundations on elastic medium. The soil property (*i.e.* elastic modulus), was modeled as a random field. The lognormal distribution was assumed for soil variability with various autocorrelation distances. The

Poisson ratio of the soil was set to be a deterministic value.

The resulting uncertainty in differential settlement due to spatial variability is evaluated by Monte Carlo simulation (MCS). Fenton and Griffiths (2002), Honjo et al. (2007), Jilati and Honjo (2008) and others have studied the influence of the spatial variability on the settlement prediction. The methodology employed in this study is similar, which was based on the random field theory (e.g. Vanmarcke, 1977, 1983) combined with the finite element method (Smith and Griffiths, 1987). However, this study was extended to show the effects of differential settlement on bending moments and stresses in a frame structure.

## 3 METHOD OF ANALYSIS

### 4 Procedure of study

Circular shallow foundations on elastic ground whose Young's modulus,  $E$ , follow a homogeneous lognormal random field were assumed. The Poisson's ratio was assumed to be constant. The settlement is calculated by the finite element method using axisymmetric condition and four nodes rectangular elements (Smith and Griffiths, 1987).

The procedure to evaluate settlement prediction uncertainty due to spatial variability is as follows:

1) A homogeneous standard normal random field was generated whose mean was zero, standard deviation was 1, and given autocorrelation distance (Shinozuka, 1971).

2) The generated Gaussian random field (RF) was transformed to the lognormal random field with given mean and standard deviation. In transforming the normal field to lognormal field, the autocorrelation distance was altered. However, it was not the exact value of the autocorrelation distance that the author was interested to study but the generated influences. The same procedure was employed in Fenton and Griffiths (2002).

3) The transformed lognormal random field was assigned to the finite element mesh. Young's modulus is assumed to be semi-isotropic (ie. no changes in the soil properties in the horizontal direction but in the vertical direction only). This assumption is justified due to much longer correlation distance to the horizontal direction compared to the vertical (e.g. Lumb, 1975). The ground's depth was 10 m discrete to 20 cm thick elements in FEM. the generated Young's modulus is assigned to each element.

4) The settlement of two independent circular foundations, differential settlement between the two circular foundations, the reaction under the foundations, and the maximum and minimum bending moment in the frame structure on the specified load were computed.

5) The steps 1 through 4 were repeated until a sufficient number of results were obtained to evaluate the uncertainty.

The procedure above was repeated for different combinations of coefficient of variation of Young's modulus,  $COV_E$ , and autocorrelation distance,  $a$ , while Poisson's ratio was assumed to be a constant ( $\nu=0.3$ ).

## 5 Derivation of the solution

The soil variability interested in was assumed to consist of a heterogeneous but isotropic RF. Although soils generally exhibit a stronger correlation in the horizontal direction compared to the vertical, due to their layered nature, the degree of anisotropy is site specific (Fenton and Griffiths, 2002) and this point will be treated in later stages. The generation procedure of a RF was described as follow (Shinozuka, 1972). The autocorrelation function of the RF was assumed to be an exponential type:

$$C(r) = \exp\left[-\frac{r}{a}\right] \quad [1]$$

where,  $C(r)$  is an autocorrelation function of an isotropic RF, and  $r$  is the distance between two points, and  $a$  is the autocorrelation distance.

Based on Wiener-Khintchine's citation, the autocorrelation function,  $C(r)$ , and the two-sided power spectrum function,  $S(\omega)$ , has the following relationships (Christakos, 1992)

$$C(r) = 2\pi \int_0^{\infty} J_0(\omega r) S(\omega) \omega d\omega \quad [2]$$

$$S(\omega) = \frac{1}{2\pi} \int_0^{\infty} J_0(\omega r) C(r) r dr \quad [3]$$

Where,  $J_0$  is Bessel function. By applying "Eq. 3" to "Eq. 1"

$$S(\omega) = \frac{1}{2\pi} \int_0^{\infty} J_0(\omega r) \exp\left[-\frac{r}{\theta}\right] r dr \quad [4]$$

On the other hand, based on Laplace - Bessel transform:

$$\int_0^{\infty} e^{-cx} x^{\alpha+1} J_{\alpha}(bx) dx = \frac{2^{\alpha+1} c b^0 \Gamma(\alpha + \frac{3}{2})}{\sqrt{\pi} (c^2 + b^2)^{\alpha + \frac{3}{2}}} \quad [5]$$

where  $\alpha$ ,  $b$ , and  $c$  are real numbers, and  $\Gamma$  is the Gamma function and it is defined as In case  $\alpha = 0$ , "Eq. 5" takes the form:

$$\int_0^{\infty} e^{-cx} x J_0(bx) dx = \frac{2 c \Gamma(\frac{3}{2})}{\sqrt{\pi} (c^2 + b^2)^{\frac{3}{2}}} \quad [6]$$

Thus

$$\Gamma(\frac{n}{2} + 1) = \sqrt{\pi} \frac{n!}{2^{(n+1)/2}} = \sqrt{\pi} \frac{1}{2}$$

So "Eq. 6" becomes:

$$\int_0^{\infty} e^{-cx} x J(bx) dx = \frac{c\sqrt{\pi}}{\sqrt{\pi} (c^2 + b^2)^{\frac{3}{2}}} \quad [7]$$

By assuming  $c=1/\theta$ ,  $b=\omega$ , and applying "Eq. 7" to "Eq. 4"

$$S(\omega) = \frac{1}{2\pi\theta \left(\frac{1}{\theta^2} + \omega^2\right)^{\frac{3}{2}}} \quad [8]$$

Based on this power spectrum function and uniform random number  $\Phi$ , a standard Gaussian random field  $Z(x_1, x_2)$  can be generated as follows:

$$Z(x_{1j_1}, x_{2j_2}) = \sum_{k_1=1}^{N_1} \sum_{k_2=1}^{N_2} a_{k_1 k_2} \cos(\omega_{k_1 k_1} x_{1j_1} + \omega_{k_2 k_2} x_{2j_2} + \Phi_{k_1 k_2}) \quad [9]$$

Where:

$$a_{k_{x_1} k_{x_2}} = \sqrt{2S(\omega)\Delta\omega_{x_1}\Delta\omega_{x_2}} \quad [10]$$

And  $(x_1, x_2)$  is the coordinate of a point in vertical plan,  $\Phi$  is a random phase angle uniformly and independently distributed in the interval  $(0, 2\pi)$ , and  $\omega_{x_1}$  and  $\omega_{x_2}$  are the considered region in the frequency domain.

## 6 COMPUTING STEPS

Step 1: Generate 2-D Gaussian random field when mean=0 and variance=1, by Monte Carlo simulation.

Consider a 2-dimensional homogeneous random field with mean zero and spectral density function  $S(\omega)$  which is insignificant magnitude outside the region defined by

$$\omega_l \leq \omega \leq \omega_u \quad [11]$$

Denote the interval vector by

$$(\Delta\omega_{x_1}, \Delta\omega_{x_2}) = \left( \frac{\omega_{x_1L} - \omega_{x_1u}}{N_{x_1}}, \frac{\omega_{x_2L} - \omega_{x_2u}}{N_{x_2}} \right) \quad [12]$$

where  $N_{x_1}$  and  $N_{x_2}$  are the numbers of the intervals along the 2 axes of the wave number domain, and  $\omega_l = -\omega_u$ , therefore the interval vector could be written as

$$(\Delta\omega_{x_1}, \Delta\omega_{x_2}) = \left( \frac{2\omega_{x_1}}{N_{x_1}}, \frac{2\omega_{x_2}}{N_{x_2}} \right) \quad [13]$$

Step 2: Transform the standard Gaussian field to a lognormal random field whose mean is  $\mu_E$  and the standard deviation is  $\sigma_E$ , as a result, only the positive value of the Young's modulus,  $E$ , are generated. The mean and variance of  $\ln E$  can be calculated as follows:

$$\sigma_{\ln E}^2 = \ln\left(1 + \frac{\sigma_E^2}{\mu_E^2}\right) \quad [14]$$

$$\mu_{\ln E} = \ln \mu_E - \frac{1}{2} \sigma_{\ln E}^2 \quad [15]$$

where  $\mu_E$  is the mean of Young's modulus, and  $\sigma_E^2$  is the variance of Young's modulus.

The procedure proposed here is extended to anisotropic case. The sample was generated in the 2 directions, and Young's modulus was assumed to be the same for the horizontal and vertical directions. However the generated field was stretched in the horizontal direction only to give longer horizontal autocorrelation distance before assigning the generated random field to the finite element mesh to be calculated (stretching by averaging the values in the horizontal direction to reach the semi-isotropic or anisotropic condition) by FORTRAN program.

Step 3: The transformed lognormal random field is assigned to the finite element mesh. Young's modulus is assumed to be the same for the horizontal direction. This assumption is justified due to much longer correlation distance to the horizontal direction compared to the vertical (e.g. Lumb, 1975). The ground's depth was 10 m discrete to 20 cm thick elements in FEM. the generated Young's modulus is assigned to each element.

Step 4: The settlements of two circular foundations, differential settlement between the two circular foundations, the support's reactions, and the maximum and minimum bending moment in the frame body on the specified load is evaluated.

Step 5: Repeat step 1 to 4 as many times as necessary.

The author considered 1000 times was sufficient in this research according to quick check for the results by comparing the predicted settlement values to the theoretical values of simulating 100, 500, 1000, or 10000 times for a case.

## 7 NUMERICAL EXAMPLE

### 8 Description of cases analyzed

The soil mass was discretized into 100x50 four-noded rectangular elements. While the overall dimensions of the ground model were  $20R$  by  $10R$ , where  $R$  was the footing radius. The size of the elements was  $0.2R$  by  $0.2R$ . The side faces of the finite element model were constrained against horizontal displacement, but were free to slide vertically; while the nodes on the bottom boundary were fixed.

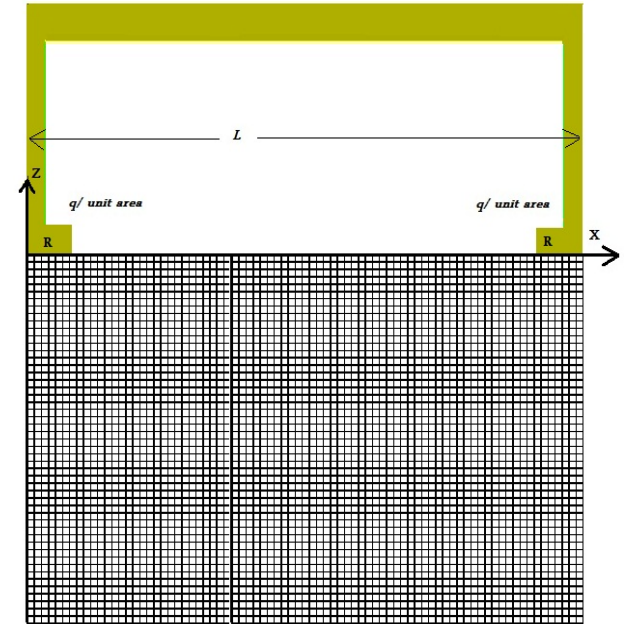


Figure 1. The ground setting and the loading conditions (none dimensional).

One might wonder if there would be boundary effects associated with such close lateral boundary; therefore, the author has evaluated the effect of the boundary condition by comparing the settlement obtained from his mesh and the settlement calculated by the Boussinesq's equations. However, it was found that a vertical displacement in each element requested by the finite element method was almost corresponding to the Boussinesq's solution, and it could be confirmed that the finite element method program used by this research was appropriate.

To generalize the results, the calculation results were normalized by  $q$  (load intensity),  $R$ , and  $L$  (the frame span) as shown in Figure 1.

The analysis was of only one footing at a time. However, the figure shows the combined case

Young's modulus,  $E$ , was given by  $E/q$ . The settlements were normalized by  $R$ , where the autocorrelation distance,  $a$ , and the differential settlements between the two footings are normalized by  $L$ . As it is shown in "table 1" 60 different combinations of parameters were examined in total. 1000 Monte Carlo simulation runs were made for each case.

Table 1. Case studied.

$E/q$	100, 150, 200
$a/L$	0.1, 0.3, 0.5, 1.0, 10
$COV_E$	0.0, 0.5, 0.7, 1.0

It could be necessary in some cases to consider the local averaging of the soil property depending on the mesh size as suggested by Vanmarcke (1977). However, it was experienced that this problem was not terribly serious in practical calculation as shown by Suzuki (1990). The problem was not further studied in detail in this study.

## 9 RESULTS AND DISCUSSION

### 10 The differential settlement between the footing's centers

Figure 2 shows the average of the differential settlement of the footing, normalized by  $L$ , against  $COV_E$ .

And figure 3 shows the average of the differential settlement of the footing, divided by the settlement of the footing on uniform ground,  $\delta^*$ , i.e.  $\Delta\delta/\delta^*$ , against  $COV_E$ .

It is observed that as the coefficient of variation of Young's modulus,  $COV_E$ , increases, the mean value of the differential settlement increases even though if the mean value of Young's modulus is the same.

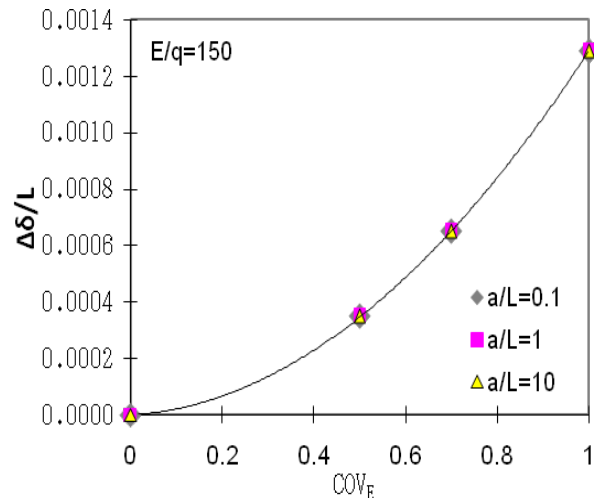


Figure 2. Relation of  $COV_E$  vs. Mean value of differential settlement.

It could be surprising that there was no difference in the mean value of the differential settlement between cases of autocorrelation distance. One would expect that a very large autocorrelation distance (ie 10 time span length) would yield much lower mean value of the differential settlement than a very small autocorrelation distance (ie. 1/10 of span length).

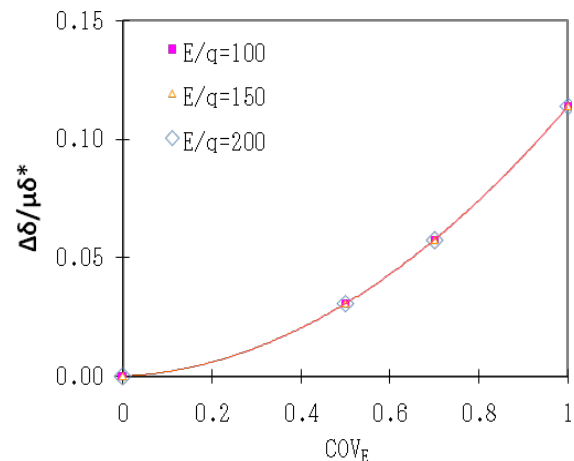


Figure 3. Relation of  $COV_E$  vs. differential settlement ratio.

Therefore, it is necessary here to call the results of some previous papers such as Fenton, and Griffiths (2002) and Honjo et al. (2007); it was found that the settlement,  $\mu\delta$ , increases as  $COV_E$  increases, however, the settlement was independent of the autocorrelation distance. That was result of assuming the horizontal autocorrelation distance to be very long and varying the vertical autocorrelation distance. Therefore, the changes in the autocorrelation distances have not affected the differential settlement either.

Also it is observed that the mean value of the differential settlement could exceed 10 % of the total settlement in case of footings on uniform ground.

### 11 The changes in the support reactions

In Figure 4 shows  $COV_E$  is plotted against  $\Delta R_a / R_a^*$ , where  $R_a^*$  is the reactions of a footing on uniform ground. It is observed that  $\Delta R_a / R_a^*$  increases as  $COV_E$  increases, and so as  $E/q$  increases.

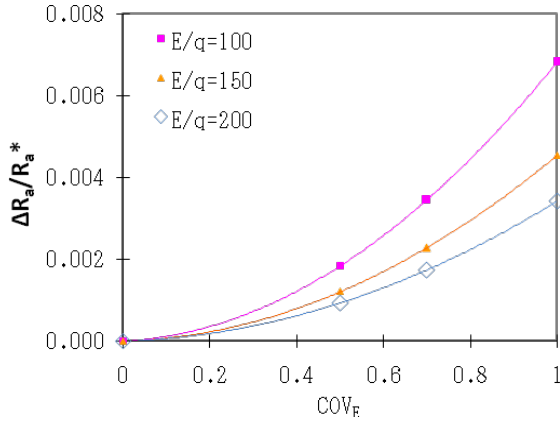


Figure 4. Relation of  $COV_E$  vs.  $\Delta R_a / R_a^*$ .

### 12 The changes in the positive bending moments

In Figure 5 shows  $COV_E$  is plotted against  $\Delta M^+ / M^{+*}$ , where  $M^{+*}$  is the maximum positive bending moment within the span results of footings on uniform ground. It is observed that  $\Delta M^+ / M^{+*}$  increases as  $COV_E$  increases, and so as  $E/q$  increases.

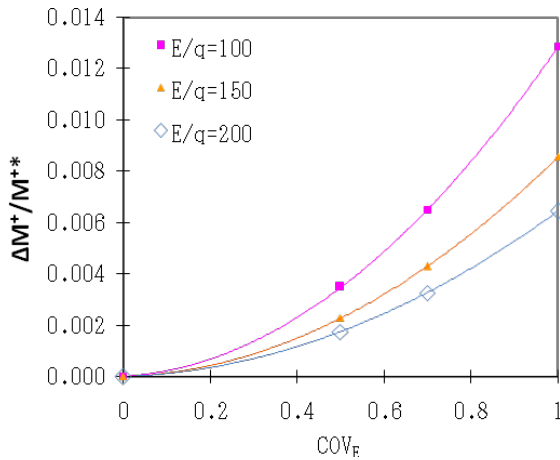


Figure 5. Relation of  $COV_E$  vs.  $\Delta M^+ / M^{+*}$ .

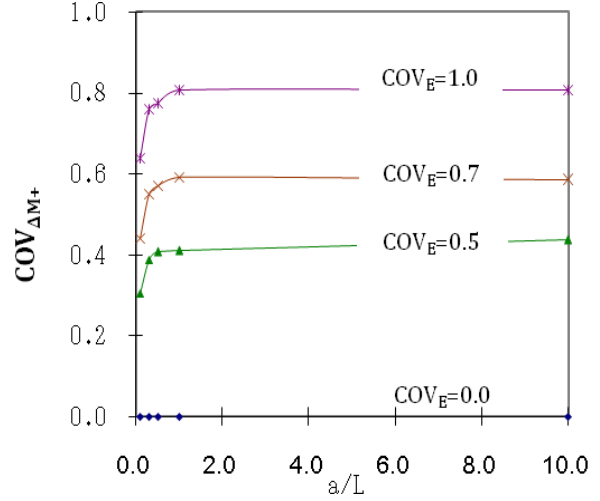


Figure 6. Relation of  $a/L$  vs.  $COV_{\Delta M^+}$ .

In Figure 6,  $a/L$  is plotted against  $COV_{\Delta M^+}$ . It is observed that  $a/L$  increases  $COV_{\Delta M^+}$  increases, however the increase is limited by  $a/L$  reaches 1. Moreover the value of  $COV_{\Delta M^+}$  ranged from 0.3 to 0.81 for  $COV_E = 0.5 \sim 1.0$ .

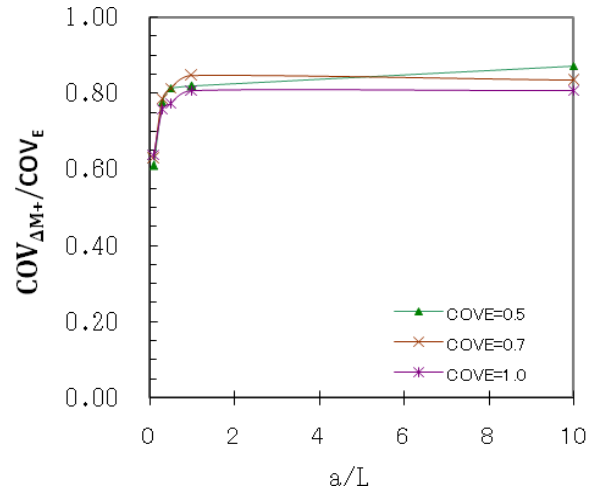


Figure 7. Relation of  $a/L$  vs.  $COV_{\Delta M^+} / COV_E$ .

In Figure 7, it is observed that as the autocorrelation distance,  $a$ , increases, the uncertainty of the predicted internal forces and stresses (i.e.  $COV_{\Delta M^+} / COV_E$ ) increases. However, it converges to 0.81- 0.87 when  $a/L$  is reaching 10.

## 13 CONCLUSIONS

The following conclusions can be drawn from this study:

It was found that as the coefficient of variation of Young's modulus,  $COV_E$ , increases, the mean value of the differential settlement increases even though the

mean value of Young's modulus is the same because the differential settlement is correlated with the heterogeneity of the spatial variability of soil ( $COV_E$ ).

Also the  $\Delta R_a / R_a^*$  and  $\Delta M^* / M^*$  are increase as  $COV_E$ , increases.

The effects of heterogeneity of the ground on the differential settlement are significant. The effect can be more than 10 % of the total settlement for  $COV_E \geq 1$  (100%). However, that have not show serious effect on the frame stresses; because the changes in  $\Delta R_a / R_a^*$  have not Exceeded 0.008 and the maximum bending moments have not Exceeded 0.014 (which is higher but still unserious or dangerous compared to the factors of safety).

It is observed that  $a/L$  increases  $COV_{\Delta M^+}$  increases, however the increase is limited by  $a/L$  reaches 1. Moreover the value of  $COV_{\Delta M^+}$  ranged from 0.3 to 0.81 for  $COV_E = 0.5 \sim 1.0$ .

It is observed that the autocorrelation distance,  $a$ , increases, the uncertainty of the predicted settlement, i.e.  $COV_{\Delta M^+} / COV_E$ , increases. However, it converges to 0.81-0.87 when  $a/L$  is reaching 10.

However, this conclusion needs for further study taking various and complicated frames.

## REFERENCES

- Fenton, G. A. and Griffiths, D. V. 2002. Probabilistic Foundation Settlement on Spatially Random Soil. *Journal of Geotechnic and Envairoment Engineering*, ASCE, 128(5):381-390.
- George Christakos. 1992. *Random Field Models in Earth Sciences*: 69-71, 325-327.
- Honjo, Y., Jililati, M. N. & Ishino, J. 2007. Effects of Spatial Variability and Statistical Estimation Error in Prediction of Settlement of a Shallow Foundation. *ICASP10 '07*, Tokyo, Japan, 1: 173-174.
- Lumb, P. 1975. Special variability of soil properties, *Proc.2nd.ICASP*:337-421
- Jililati, M. N. and Honjo, Y 2008. Effects of Spatial Variability of soil parameters on settlement of a Shallow Foundation. *Journal of Theoretical and Applied Mechanics*, (57): 49-56.
- Shinozuka, M. 1972. Digital simulation of random processes and its applications. *Journal of sound and vibration*, 25(1):111-128.
- Shinozuka, M. 1971. Simulation of multivariate and multi dimensional random processes. *Journal of Acoustical Society of America*, 49(1) (Part2): 357-367.
- Smith, I. M and Griffiths D. V. 1987. *Programming the Finite Element Method*. pp.182-186, John Wiley & Sons
- Suzuki, M. 1990. *Probabilistic description of spatial distribution characteristics of geotechnical parameters and basic study on geotechnical reliability design*. Doctoral thesis submitted to Nagoya Institute of Technology.
- Thoft-Chiridtsen, P. and M. J. Baker 1982. *Structural Reliability Theory and Its Application*, Springer-Verlag.
- Vanmarcke, E. H. 1983. Random Field: analysis and synthesis, *The MIT press*.

Vanmarcke, E. H. 1977. Probabilistic modeling of soil profiles. *Journal of Geotechnical Engineering*, ASCE, 103(GT11):1227-1